

Fabricating Multi-Material Nanofabrics using Rotary Jet Spinning*

Nina R. Sinatra, Johan U. Lind, and Kevin Kit Parker

Abstract—Multi-material nanofiber composites have recently attracted attention, as they introduce new opportunities for regulating mechanical, electrical, and biological properties. Here we present a novel manufacturing method for multi-material composite nanofabrics. Using infrared spectroscopy and tensile testing, we compare the mechanical and structural properties of multi-material fabrics and single fiber blends. We find that multi-material nylon/polyurethane fabrics are tougher than their pure components, and that mechanical properties of composite nanofabrics can be tuned by varying the polymer ratio and composition. The capability of this system to fabricate nanotextiles using orthogonal solvents is also demonstrated.

I. INTRODUCTION

Nanofibers have been explored as a basis for various applications, including sensing and catalysis [1], tissue engineering [2, 3], and textiles [4, 5], due to their high specific surface area and unique manufacturing parameters. Nanofiber composite textiles based on two or more distinct fiber types would facilitate tuning material, physical, and chemical properties, and combining base materials that require the use of immiscible solvents. On the microscale, reinforcing fibrous constructs with fibers of disparate elastic moduli is used to control the elastic modulus (resistance to elastic deformation) and toughness (ability to absorb energy without fracturing) of the composite structure [6, 7]. Integrating multiple types of polymer fibers at the nanoscale will enable the development of scaffolds whose toughness and elasticity can be easily regulated through material selection and the ratio of components.

However, current fiber fabrication techniques are challenged by applications requiring multi-phase nanotextiles or orthogonal solvents. Recent approaches to fabricating multi-material nanotextiles are either limited to adjoining biphasic (Janus-type) fibers [8], constrained by charge interference from adjacent spinnerets [9], or produce highly delineated sheets rather than well-integrated multi-modal textiles [10]. These arrangements limit customizability of the final nanofabric by requiring the use of similar solvents and processing parameters for both solutions [11]. The centrifugal force-based rotary jet spinning (RJS) system has the potential to overcome these limitations by eliminating the reliance on electric fields for fiber formation and reducing the number of processing parameters [5, 12, 13].

Here, we describe the fabrication of tough multi-material polymer nanofabrics using a custom-designed dual chamber RJS reservoir. We study the influence of reservoir chamber and nanofabric composition on fiber structural and mechanical properties, respectively. Our results show that composite multi-material nanofabrics are tougher than either individual

component, as well as single fiber blends of both materials. Further, both polymers are heterogeneously distributed across a composite nanofiber sheet. Finally, we demonstrate that this method can be used to manufacture multi-modal nanotextiles from distinct polymers that require the use of orthogonal solvents.

II. EXPERIMENTAL SETUP

A. Materials

Precursor solutions for nanofiber fabrication were prepared by dissolving nylon (Nylon 6, Sigma-Aldrich, St. Louis, MO), polyurethane (Lubrizol, Cleveland, OH) and/or polyethylene terephthalate (PET, McMaster-Carr, Princeton, NJ) in 1,1,1,3,3,3-hexafluoro-2-propanol (Sigma-Aldrich, St. Louis, MO). Poly(vinylidene fluoride-co-trifluoroethylene) (PVDF-TrFE, Sigma-Aldrich, St. Louis, MO) solutions were prepared using dimethylformamide (DMF, Sigma-Aldrich, St. Louis, MO) and acetone (Avantor Performance Materials, Center Valley, PA) as solvents.

B. Reservoir Design and Fiber Fabrication

The RJS system consists of a brushless DC servo motor (Maxon Motor Company, Fall River, MA) attached to a custom-designed aluminum reservoir rotating at 30,000 rpm. The single chamber reservoir contains one 340 μm sidewall orifice. The dual chamber reservoir (DCR) consists of two concentric cavities, each containing a 500 μm aperture. Infusion rate of precursor solutions into the reservoir was regulated using an external syringe pump. All solutions were infused at a constant rate of 5 mL min^{-1} . Fibers were collected on a rotating cylindrical collector (3000 rpm) mounted on a linear motor.

C. Fiber Image Analysis

Various concentrations of polymer nanofibers were sputter coated using an Au target (Denton Vacuum, Moorestown, NJ), and then imaged using a field emission scanning electron microscope (Carl Zeiss, Dresden, Germany). Image analysis was performed using ImageJ software (National Institutes of Health, Bethesda, MD). 300 fibers were analyzed, including 4 random fields of view (FOVs) per sample and 3 samples per condition.

D. Mechanical Characterization of Fibers

A uniaxial tension test (CellScale BioTester, Waterloo, ON, Canada) was used to measure the mechanical properties of nanofiber sheets in air. Prior to each test, the thickness, width, and gauge length of the fiber sample were recorded using a micrometer.

*Research supported by NSF (DMR-1420570). The authors are with the John A. Paulson School of Engineering and Applied Sciences, Harvard University, Cambridge, MA, 02138, USA, and the Wyss Institute for

Biologically Inspired Engineering, Harvard University, Boston, MA, 02115, USA. (email: nsinatra@fas.harvard.edu, jlind, kkparker@seas.harvard.edu)

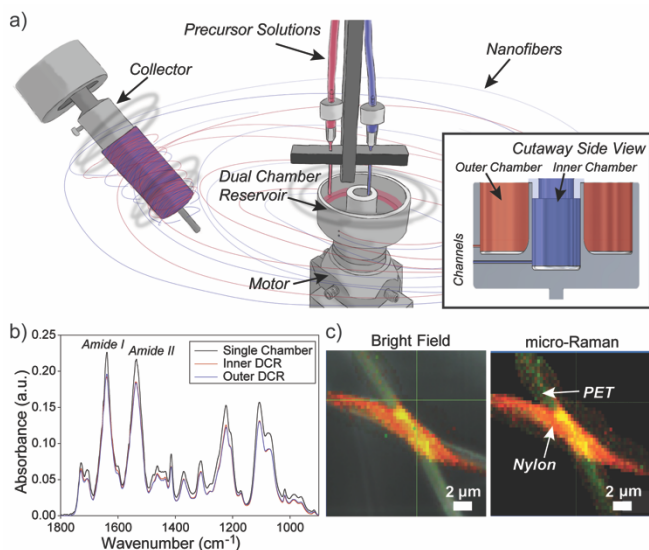


Figure 1. a) Illustration of multi-material nanofabric fabrication using rotary jet spinning (RJS) and the dual chamber reservoir (DCR). *Inset*: Cutaway side view of the DCR. Inner and outer chambers are denoted in blue and red, respectively. b) FTIR spectra of single and dual chamber nanofabrics. Data are averaged for $n = 3$ production runs per condition, with 16 random FOVs per sample. c) Bright field with spectra overlay and micro-Raman images displaying distinct nylon and PET nanofibers. The nylon and PET nanofibers are indicated in red and green, respectively.

E. Fourier Transform Infrared (FTIR) Spectroscopy

Infrared spectra of nanofabric samples were recorded in air using Fourier transform infrared spectroscopy (Bruker Lumos FTIR microscope, Billerica, MA) using the attenuated total reflectance (ATR) technique. A resolution of 4 cm^{-1} and 16 scans was used for both local spectra sampling and 2D contour mapping. For contour mapping, data was normalized to maximum intensities.

F. Micro-Raman Spectroscopy

Raman spectra of nanofiber samples were acquired in air using a confocal Raman microscope (LabRAM HR Evolution, Horiba Scientific, Edison, NJ). A 532 nm Ar-ion laser was used to excite the sample with a 100x objective. The spectra were processed using LabSpec 6 software.

F. Statistical Analysis

All error was reported as standard error of the mean (SEM). Analysis of variance (ANOVA) tests were performed during statistical comparisons. P -values below 0.05 were considered statistically significant.

III. RESULTS

A. Fiber Structure Conserved across Reservoirs

We developed a dual chamber reservoir (DCR, Fig. 1a) to fabricate multi-material nanofabrics using rotary jet spinning. The reservoir contains circular (inner) and annular (outer) compartments, which are separated and vertically offset to prevent solution mixing (Fig. 1a, inset). The sidewall apertures of the two chambers are aligned vertically relative to each other to limit contact of nanofiber jets during fiber fabrication. Precursor solutions of nylon-6 and polyurethane (PU) in 1,1,1,3,3,3-hexafluoro-2-propanol (HFIP) were

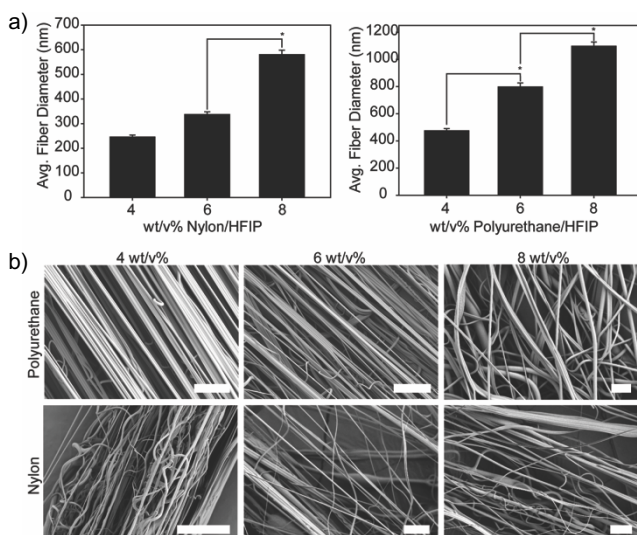


Figure 2. a) Average diameter and b) Scanning electron images of nylon and polyurethane nanofibers spun at 4 wt/v%, 6 wt/v%, and 8 wt/v% in HFIP. Data are averaged for $n = 3$ production runs per condition, 3 samples per run, and 300 fibers across 4 FOVs. * indicates $p < 0.05$. All scale bars: $10\ \mu\text{m}$.

simultaneously infused into the DCR and were continually fed during fiber manufacture. (Fig. 1a). During high speed reservoir rotation, centrifugal force propels each solution through its respective orifice. As these polymer jets elongate and the volatile solvent evaporates, two discrete nanofibers are formed and accumulate on a rotating collector (Fig. 1a).

First, we asked whether the choice of DCR chamber (inner or outer) influenced nanofiber structure, and whether these fibers differed from those fabricated by the single chamber reservoir used in previous RJS studies [12]. A blended 5 wt/v% nylon / 5 wt/v% PU solution was injected individually into the inner and outer DCR chambers. Fourier transform infrared spectroscopy (FTIR) was used to assess the structural properties of polymer nanofibers as a function of the DCR fabrication process. Vibrational peaks corresponding to both nylon (Amide I, 1641 cm^{-1}) and PU (Amide II, 1547 cm^{-1}) are evident in the spectra recorded for nanofibers fabricated using both chambers (Fig. 1b). No peak shifts are observed between spectra acquired for the inner and outer chambers, indicating no significant differences between the structure of polymer nanofibers fabricated using either compartment. Further, FTIR verified that DCR fiber fabrication does not significantly affect the structural properties of nylon/PU nanofabrics, in comparison with the conventional single chamber reservoir (Fig. 1b).

In a similar test, a multi-material nanofabric was manufactured by simultaneously infusing a 10 wt/v% nylon solution into the inner DCR chamber and a 5 wt/v% PET solution into the outer chamber, both using HFIP as the solvent. Micro-Raman spectroscopy confirmed that both nylon and PET nanofibers were independently present in a composite multi-material nanofabric (Fig. 1c). Collectively, these results indicated that fiber formation was consistent across both channels, no structural artifacts were introduced during chamber selection, and distinct polymer nanofibers were produced from each chamber.

B. Fabric Composition Influences Material Mechanics

We then investigated the impact of nanofabric composition on network mechanical properties by comparing the toughness and specific elastic modulus of multi-material, blend, and single-component polymer nanofibers. Nylon and polyurethane were selected for this analysis based on the significant difference between their elastic moduli. First, the concentration of nylon and PU solutions was varied from 4 to 8 wt/v% in HFIP in increments of 2 wt/v%, and nanofiber diameter was measured for each condition (Fig 2a-b). Next, multi-material nanofabrics were manufactured by infusing a 6 wt/v% PU solution into the inner DCR chamber, and a 6 wt/v% nylon solution into the outer chamber. Single fiber polymer blends were fabricated by mixing nylon and PU into one 6 wt/v% solution. As a control, pure 6 wt/v% nylon and pure 6 wt/v% PU nanofibers were each spun individually using the outer and inner DCR compartments, respectively. The samples were loaded uniaxially until failure at a constant elongation rate of 8 mm min⁻¹.

Multi-material nylon/PU nanofabrics manufactured using this technique are tougher than either material alone (Fig. 3a). Equally important, they displayed increased specific elastic modulus (Fig. 3b), in comparison with single fiber polymer blends. Moreover, these parameters can be tuned by adjusting the concentration and relative ratio of each component in a multi-modal nanofabric. Because 4-6 wt/v% solutions yielded nanoscale fibers for both polymers, these concentrations were used to assess the influence of polymer ratio on network mechanical properties. Using various combinations of 4 wt/v% and 6 wt/v% nylon and PU solutions, the nylon:PU ratio in multi-material samples was varied from 1:1 to 3:2 and 2:3. Due to the higher toughness and lower elastic modulus of PU relative to nylon, we predicted that higher concentrations of the elastomer would increase the toughness and decrease the tensile modulus of the overall composite. As expected, multi-material fabrics with a lower nylon:PU ratio and larger PU nanofibers exhibited higher toughness and lower specific

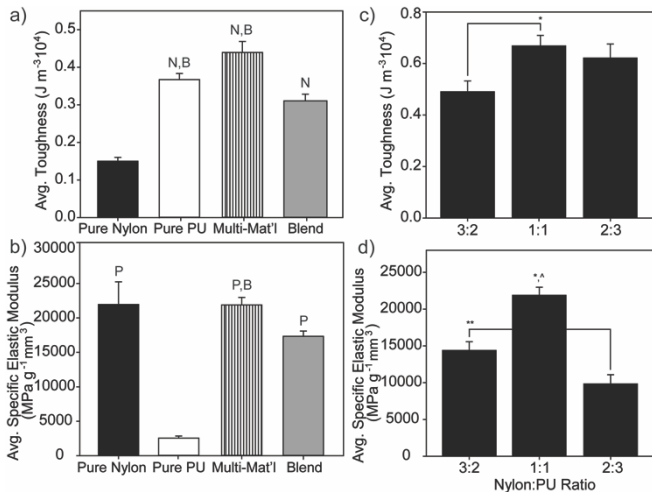


Figure 3. Comparative a) toughness and b) specific elastic modulus of pure nylon and PU, single fiber Nylon/PU blend, and multi-material Nylon/PU nanofabrics. Varying Nylon/PU ratio and concentration enables us to tune the c) toughness and d) specific elastic modulus of a multi-material nanofabric. *, **, N, B, and P indicate $p < 0.05$. N, B, and P denote significant difference from Pure Nylon, Pure PU, and Blend, respectively. For all conditions, $n = 3$ production runs and 3 samples per run.

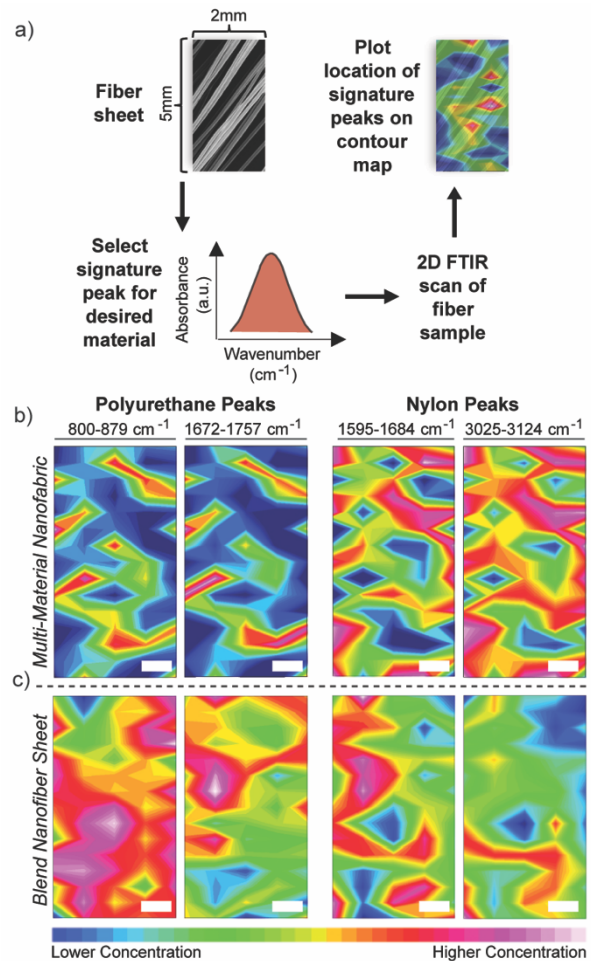


Figure 4. a) Schematic of experimental setup used to analyze dispersion of polymer components in nanofabrics. 2D FTIR contour maps of Nylon and PU dispersion in b) multi-material nanofabrics and c) blend nanofibers. The normalized intensity is indicated using a color gradient. Red regions signify higher polymer concentrations, while blue indicates lower concentrations. For each condition, $n = 3$ production runs, with $n = 3$ samples and 75 FOVs per sample. Representative contour maps are shown. Scale bars: 0.5 mm.

elastic moduli than those with higher ratios or thinner elastomer fibers (Fig. 3c-d).

The difference in mechanical properties between single fiber blends and multi-material composite samples may be influenced by whether nylon and PU are both localized in each fiber (blend) or in separate fibers (multi-material). To further explore the dispersion pattern of both polymers in a nanofiber sheet, we used FTIR to generate 2D contour maps. Two characteristic vibrational modes for nylon and for PU were selected, and the intensity of these peaks was recorded to map the location of each polymer across 75 regions of interest on a 10 mm² nanofiber sheet (Fig. 4a). The normalized intensity of each polymer at a given location was illustrated using a color gradient from red to blue, with red indicating higher polymer concentrations and blue denoting lower local concentrations. In our analysis, 2D FTIR contour maps indicate that nylon and PU nanofibers are well-integrated in the multi-material sheet (Fig. 4b), and suggest that their dispersion is more heterogeneous on the network level than in the blend sheet (Fig. 4c). This stratification may account for the higher

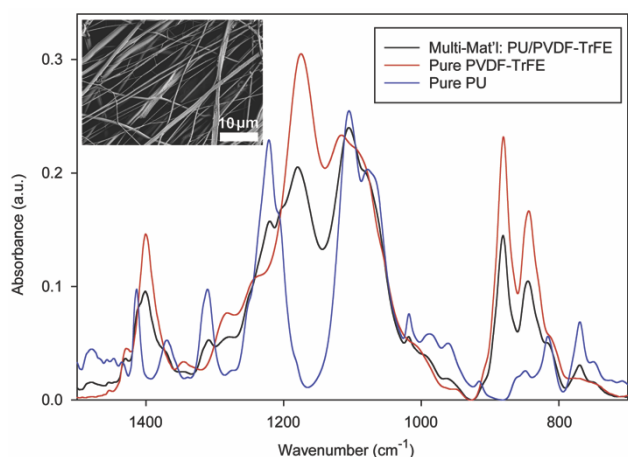


Figure 5. FTIR spectra of pure PVDF-TrFE, pure PU, and multi-material PVDF-TrFE/PU nanofabrics. Data are averaged for $n = 3$ samples, with 16 FOVs per sample. *Inset*: Scanning electron micrograph of multi-material PVDF-TrFE/PU nanofabric.

toughness of the multi-material nanofabric by facilitating load transfer from stiffer nylon fibers to more elastic PU fibers.

C. Manufacturing Composite Nanofabrics using Orthogonal Solvents

Finally, we asked whether the DCR could be used to fabricate multi-material nanotextiles using orthogonal solvents. To explore this question, we chose the piezoelectric co-polymer PVDF-TrFE as a proof of concept. Unlike nylon and polyurethane, PVDF-TrFE has limited solubility in most of the organic solvents used for RJS. Moreover, although the co-polymer is less brittle than more commonly used inorganic piezoelectric ceramics (e.g. lead zirconate titanate), many PVDF-TrFE-based sensors rely on sandwiching nanofiber mats between elastic sheets to increase flexibility [14]. Thus, by producing a composite nanofabric using PVDF-TrFE and PU, this method has the potential to preserve the piezoelectricity of the co-polymer while incorporating an elastomer on the nanoscale as a mechanical support.

Precursor solutions of 6 wt/v% PU in HFIP and 15 wt/v% PVDF-TrFE in DMF:acetone (1:1) were infused into the inner and outer DCR chambers, respectively. Relevant vibrational modes of PVDF-TrFE (crystalline β phase, 840 cm^{-1}) and PU (C-O-C stretch, 1162 cm^{-1}) were examined using FTIR. Composite nanofabric spectra were compared to those of pure PU nanofibers and of PVDF-TrFE cast films (Fig. 5). Both characteristic peaks are present in the multi-material PU/PVDF-TrFE nanofabrics, indicating the presence of both types of polymer nanofibers. This data suggests the ability of this technique to fabricate composite nanofabrics using two materials with orthogonal solvents. Future research may investigate the mechanical and electrical properties of PU/PVDF-TrFE composites and explore the impact of component ratio on bulk piezoelectricity.

IV. CONCLUSION

We have demonstrated a novel technique to manufacture multi-material polymer nanofabrics using rotary jet spinning. Taken collectively, our data suggest that adding a dual chamber reservoir to the RJS system provides three key advantages for fiber fabrication: (1) mechanical properties can

be controlled by tuning the ratio and concentration of each component, (2) both fiber types are well dispersed throughout the nanofabric, and (3) multiple polymers can be spun into the same nanofabric regardless of solvent compatibility (e.g. orthogonal solvents can be used for each individual material). This method simplifies the process of generating multi-phase nanofabrics using two polymers and/or immiscible solvents. Future studies could exploit this capability to fabricate multi-material nanofiber scaffolds, flexible sensors, and lightweight devices by combining electronic, elastic, or drug-eluting materials.

V. ACKNOWLEDGMENT

The authors appreciate the support of the Wyss Institute for Biologically Inspired Engineering and the Harvard John A. Paulson School of Engineering and Applied Sciences. This work was performed in part at the Center for Nanoscale Systems (CNS), a member of the National Nanotechnology Infrastructure Network (NNIN), which was supported by the National Science Foundation (Award No. ECS-0335765). The authors gratefully acknowledge the graphic artwork provided by Karaghen Hudson, the assistance of Dr. Arthur McClelland with micro-Raman spectroscopy measurements, and the helpful comments of Dr. John Zimmerman.

REFERENCES

- [1] S. Thenmozhi, N. Dharmaraj, K. Kadirvelu, and H. Y. Kim, "Electrospun nanofibers: New generation materials for advanced applications," *Materials Science and Engineering: B*, vol. 217, pp. 36-48, 2017.
- [2] A. Capulli, L. MacQueen, S. P. Sheehy, and K. Parker, "Fibrous scaffolds for building hearts and heart parts," *Advanced drug delivery reviews*, vol. 96, pp. 83-102, 2016.
- [3] V. Malkoc and L. Chang, "Applications of electrospun nanofibers in neural tissue engineering," *European Journal of BioMedical Research*, vol. 1, pp. 25-29, 2015.
- [4] L. F. Deravi, N. R. Sinatra, C. O. Chantre, A. P. Nesmith, H. Yuan, S. K. Deravi, *et al.*, "Design and Fabrication of Fibrous Nanomaterials Using Pull Spinning," *Macromolecular Materials and Engineering*, vol. 302, 2017.
- [5] G. M. Gonzalez, L. A. MacQueen, J. U. Lind, S. A. Fitzgibbons, C. O. Chantre, I. Huggler, *et al.*, "Production of Synthetic, Para-Aramid and Biopolymer Nanofibers by Immersion Rotary Jet-Spinning," *Macromolecular Materials and Engineering*, 2016.
- [6] N. Pan, "Development of a Constitutive Theory for Short-fiber Yarns. Part IV: The Mechanics of Blended Fibrous Structures," *Journal of the Textile Institute*, vol. 87, pp. 467-483, 1996.
- [7] S. Ghosh and L. Chapman, "Effects of fiber blends and needling parameters on needlepunched moldable nonwoven fabric," *Journal of the Textile Institute*, vol. 93, pp. 75-87, 2002.
- [8] A. Khang, P. Ravishankar, A. Krishnaswamy, P. K. Anderson, S. G. Cone, Z. Liu, *et al.*, "Engineering anisotropic biphasic Janus-type polymer nanofiber scaffold networks via centrifugal jet spinning," *Journal of Biomedical Materials Research Part B: Applied Biomaterials*, 2016.
- [9] S.-P. Fang, P. Jao, D. E. Senior, K.-T. Kim, and Y.-K. Yoon, "Study on high throughput nanomanufacturing of photopatternable nanofibers using tube nozzle electrospinning with multi-tubes and multi-nozzles," *Micro and Nano Systems Letters*, vol. 5, p. 10, 2017.
- [10] S. Senturk-Ozer, S. Aktas, J. He, F. T. Fisher, and D. M. Kalyon, "Nanoporous nanocomposite membranes via hybrid twin-screw extrusion—multijet electrospinning," *Nanotechnology*, vol. 28, p. 025301, 2016.
- [11] S. P. Adhikari, G. P. Awasthi, H. J. Kim, C. H. Park, and C. S. Kim, "Electrospinning Directly Synthesized Porous TiO₂ Nanofibers Modified by Graphitic Carbon Nitride Sheets for

- Enhanced Photocatalytic Degradation Activity under Solar Light Irradiation," *Langmuir*, vol. 32, pp. 6163-6175, 2016.
- [12] M. R. Badrossamay, H. A. McIlwee, J. A. Goss, and K. K. Parker, "Nanofiber assembly by rotary jet-spinning," *Nano letters*, vol. 10, p. 2257, 2010.
- [13] H. M. Golecki, H. Yuan, C. Glavin, B. Potter, M. R. Badrossamay, J. A. Goss, *et al.*, "Effect of Solvent Evaporation on Fiber Morphology in Rotary Jet-Spinning," *Langmuir: the ACS journal of surfaces and colloids*, vol. 30, p. 13369, 2014.
- [14] H. B. Lee, Y. W. Kim, J. Yoon, N. K. Lee, and S.-H. Park, "3D customized and flexible tactile sensor using a piezoelectric nanofiber mat and sandwich-molded elastomer sheets," *Smart Materials and Structures*, vol. 26, p. 045032, 2017.